JES

JOURNAL OF ENVIRONMENTAL SCIENCES

ISSN 1001-0742
CN 11-2629/X

July 1, 2013 Volume 25 Number 7
www.jesc.ac.cn

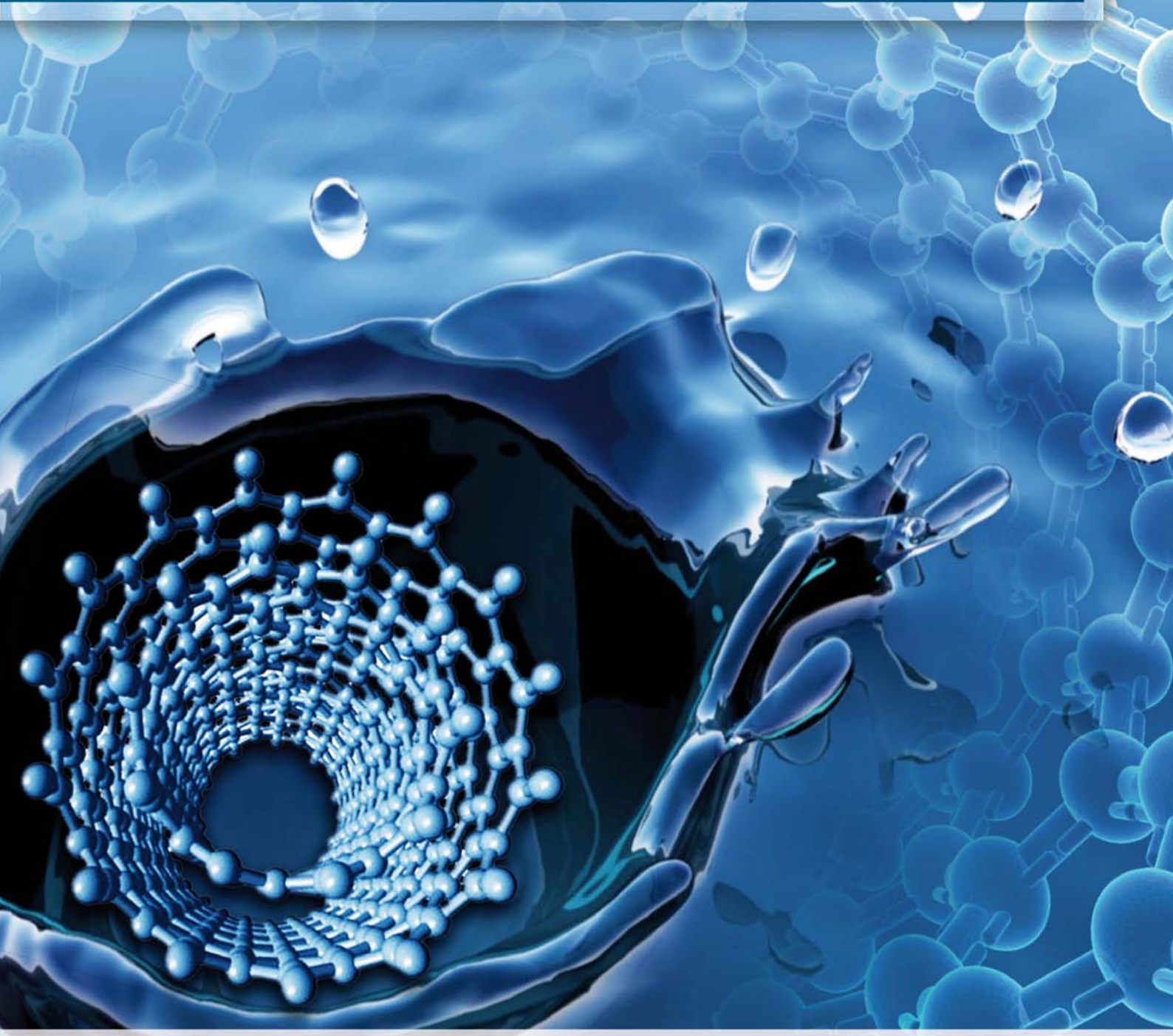

ELSEVIER

Science Press

Sponsored by
Research Center for Eco-Environmental Sciences
Chinese Academy of Sciences

ISSN 1001–0742 **Journal of Environmental Sciences** Vol. 25 No. 7 2013

CONTENTS

Environmental health and toxicology

Environmental catalysis and materials

The 8th International Conference on Sustainable Water Environment

Serial parameter: CN 11-2629/X*1989*m*237*en*P*28*2013-7

Available online at www.sciencedirect.com
ScienceDirect
Journal of Environmental Sciences 2013, 25(7) 1331–1337
JOURNAL OF ENVIRONMENTAL SCIENCES
ISSN 1001-0742
CN 11-2629/X
www.jesc.ac.cn

A pilot-scale study of cryolite precipitation from high fluoride-containing wastewater in a reaction-separation integrated reactor

Ke Jiang, Kanggen Zhou*, Youcai Yang, Hu Du

School of Metallurgical Science and Engineering, Central South University, Changsha 410083, China.
E-mail: j_k8663661@126.com

Received 17 October 2012; revised 04 February 2013; accepted 06 February 2013

Abstract

Fluoride removal by traditional precipitation generates huge amounts of a water-rich sludge with low quality, which has no commercial or industrial value. The present study evaluated the feasibility of recovering fluoride as low water content cryolite from industrial fluoride-containing wastewater. A novel pilot-scale reaction-separation integrated reactor was designed. The results showed that the seed retention time in the reactor was prolonged to strengthen the induced crystallization process. The particle size of cryolite increased with increasing seed retention time, which decreased the water content. The recovery rate of cryolite was above 75% under an influent fluoride concentration of 3500 mg/L, a reaction temperature of 50°C, and an influent flow of 40 L/hr. The cryolite products that precipitated from the reactor were small in volume, large in particle size, low in water content, high in crystal purity, and recyclable.

Key words: fluoride-containing wastewater; cryolite; crystallization; low water content; reaction-separation integrated reactor

DOI: 10.1016/S1001-0742(12)60204-6

Introduction

In various industries, including the production of fluoride salts, large amounts of fluoride-containing wastewater with a high fluoride concentration are produced. Fluoride wastewater is a typical effluent due to the hazardous effects such as mottling of teeth, softening of bones, and ossification of tendons and ligaments (Reardon and Wang, 2000). The conventional method for fluoride removal generally involves chemical precipitation and coagulation (Wu and Lu, 2003; Turner et al., 2005; Meenakshi and Maheshwari, 2006). However, due to its high water content and low quality, the sludge has no commercial or industrial value and has to be disposed with increasing costs (Aldaco et al., 2005; Kristel et al., 2003).

In 2009, the world fluorspar reserves were estimated at 230 million tons. The worldwide consumption of "acid grade" fluorspar is currently approximately 4 million tons per year (Aldaco et al., 2007). The known reserves are estimated to be adequate to approximately 50 years supply. Hence, the recovery of fluoride from industrial wastewater is presented as an important target of the fluorine industry.

As important raw materials of fluoride salt, calcium fluoride and cryolite can be precipitated from fluoride-containing wastewater by adding calcium salt (Eq. (1)) or sodium aluminate (Eq. (2)), respectively.

$$Ca^{2+}+2F^{-}= CaF_2 \quad (1)$$

$$3Na^{+}+Al^{3+}+6F^{-}= Na_3AlF_6 \quad (2)$$

The traditional stirred tank reactor and fluidized bed reactor are widely used for calcium fluoride recovery. The calcium fluoride recovered in the traditional stirred tank reactor could not be dehydrated and reused economically due to its high water content and fine particle size (Lee et al., 2001). The fluidized bed reactor is developed based on the crystallization process (Aldaco et al., 2007; Hirasawa et al., 2002; Corre et al., 2009). The water content of sludge is greatly decreased while the seed retention time is prolonged. However, the optimal hydraulic retention time and fluidization state of seed, which are both determined by influent flow, are difficult to control. Moreover, the recovery of calcium fluoride from wastewater with high concentrations of aluminum and fluoride is not feasible (Jiang et al., 2012). Therefore, an alternative option is to recover cryolite instead of calcium fluoride (Wang et al., 2012; Shi et al., 2012). However, little attention has been paid to the crystallization process of cryolite.

This study aims to recover cryolite with low water content and large particle size cryolite from a high fluoride-

* Corresponding author. E-mail: zhoukg63@163.com

containing wastewater by the crystallization process. A novel pilot-scale reactor called reaction-separation integrated reactor was designed. Continuous experiments were carried out to validate the feasibility of the process.

1 Materials and methods

1.1 Materials

Both synthetic wastewater and industrial wastewater were used as influent. The synthetic wastewater (2700 mg/L) was prepared with hydrofluoric acid (HF, analytical grade). The industrial wastewater was obtained from a fluoride chemical factory in Hunan Province, China. The detailed composition of the industrial wastewater are as following (mg/L): F 3500, Mg 340, Al 60, S 120, K 210, Si 590, Na 1090 and Ca 40 mg/L, pH = 2.5. The precipitant of cryolite, sodium aluminate, was prepared by dissolving industrial-grade aluminium hydroxide ($Al(OH)_3$) and sodium hydroxide (NaOH) at 90°C. The molar ratio of sodium oxide (Na_2O) to aluminum oxide (Al_2O_3) in sodium aluminate was defined as α_k.

1.2 Reactor design and process description

The reactor consisted of a polypropylene cylindrical vessel (40 L), a deceleration mixer, a cubic container (100 L), an electric heater, and two pumps. The cylindrical vessel was divided into an inner space (200 mm × 600 mm) and an outer space (315 mm). During operation, the wastewater and precipitant were added into the inner space from the top of the reactor. The F/Al molar ratio and reaction pH were adjusted by the flow of precipitant. The deceleration mixer was used to mix the wastewater and precipitant, which was different from the fluidized bed reactor. The temperature was controlled by the electric heater and thermostats. When the reaction solution flowed into the outer space, the turbulence of solution was decreased under the action of a clapboard. Subsequently, the solid phase retained on the bottom of the reactor, and the liquid phase flowed out of the reactor from the outlet. The schematic of the reactor is shown in **Fig. 1**. The operation conditions are shown in **Table 1**.

Table 1 Operational conditions in the pilot-scale experiments

Operational conditions	Run 1	Run 2	Run 3	Run 4
Wastewater	Synthetic wastewater	Synthetic wastewater	Synthetic wastewater	Industrial wastewater
Influent flow of wastewater (L/hr)	40	40	20–80	40
Reaction pH	3.0–9.0	3.0–9.0	5.0–7.0	2.5–7.0
α_k	3.00	3.00	3.00	1.88–3.25
Temperature (°C)	50	30–60	50	35–50

α_k: molar ratio of sodium oxide (Na_2O) to aluminum oxide (Al_2O_3) in sodium aluminate.

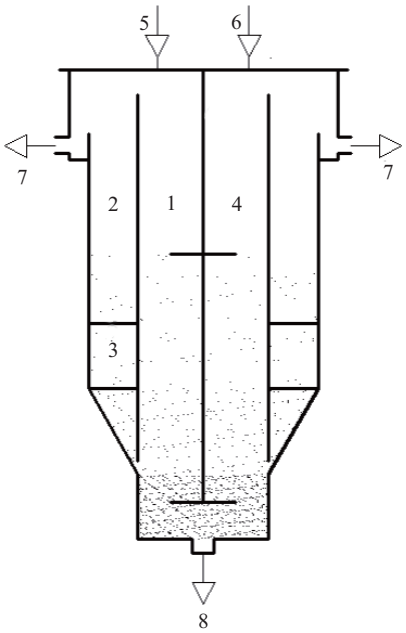

Fig. 1 Schematic of the pilot-scale reactor for recovery of cryolite. (1) inner space; (2) out space; (3) clapboard; (4) deceleration mixer; (5) wastewater inlet; (6) precipitant inlet; (7) effluent outlet; (8) cryolite outlet.

1.3 Sampling and analysis

The effluent was sampled from the outlet every 0.5 hr. The wet samples of cryolite were sampled from the outlet on the bottom of the reactor. The residual fluoride concentration of the effluent was measured by ion-selective electrodes. The wet samples of cryolite were dried at 40°C for 10 hr. The hygroscopic water of dry samples was determined by standard of YS/T273.1-200 (China). Dry samples of cryolite were analyzed by X-ray diffraction (XRD, TTR III, Japan), X-ray photoelectron spectroscopy (ZSX Primus II, Japan), and scanning electron microscopy (SEM, JSM 6360LV, Japan). The arithmetic mean particle size of cryolite was measured by a computer program Smile View based on the SEM image.

Water content of wet samples (w) was determined by Eq. (3):

$$w = (m_1 - m_2)/m_1 \times 100\% \quad (3)$$

where, m_1 (g) and m_2 (g) are the masses of wet and dry samples, respectively. The recovery of cryolite (R) was defined by Eq. (4):

$$R = (F_{in} \times C_{in} - F_{out} \times C_{out})/F_{in} \times C_{in} \quad (4)$$

where, C_{in} (mg/L) and C_{out} (mg/L) are the fluoride concentration of the influent and effluent, respectively; and F_{in} (L/hr) and F_{out} (L/hr) are the flow of the influent and effluent, respectively. The stirring reaction time of cryolite (t, hr) was defined by Eq. (5):

$$t = F_{in}/V_1 \quad (5)$$

where, V_1 (L) is the volume of inner space in the reactor. The molar ratio of the cryolite product was defined as Na/Al molar ratio.

The cryolite products recovered from the traditional stirred tank reactor in a fluoride chemical factory were sampled and analyzed for comparison.

2 Results and discussion

2.1 Recovery of cryolite from synthetic wastewater

2.1.1 Influence of F/Al molar ratio on the recovery rate of cryolite

Figure 2 shows the influence of F/Al molar ratio on the recovery rate of cryolite and reaction pH (Run 1). The reaction pH increases with decreasing F/Al molar ratio. This result can be explained by the constitution of the influent and the precipitant. As shown in Section 1.1, the H/F molar ratio in the influent is 1:1, and the OH/Al molar ratio in the precipitant is 6:1 at α_k = 3.00. Under this condition, the reaction pH is determined indirectly by the F/Al molar ratio. Therefore, we use reaction pH as a parameter to estimate the F/Al molar ratio trend while maintaining constant α_k and wastewater matrix.

At pH 3.0 to 4.0, the recovery rate of cryolite increases with decreasing F/Al molar ratio. At pH 4.0 to 8.0, the recovery rate reaches 75% to 80% with corresponding F/Al molar ratio from 2.7 to 6.0. This result indicates that the dosage of the precipitant is sufficient. At pH 8.0 to 9.0, the recovery rate of cryolite slightly decreases, which may be attributed to the fact that the concentration of free Al^{3+} ions decreases when $Al(OH)_3$ precipitates in the solution at high pH (Chang, 2008).

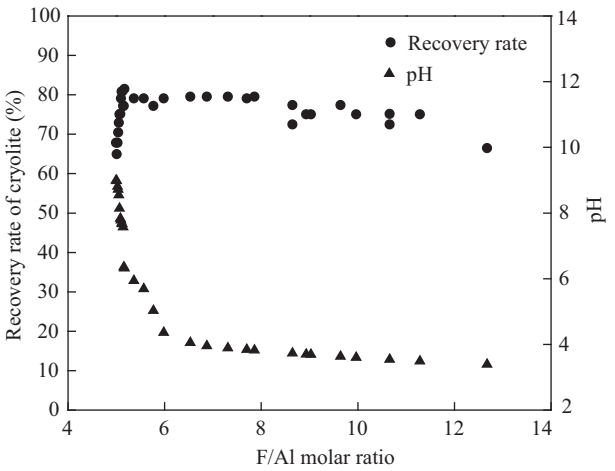

Fig. 2 Influence of F/Al molar ratio on the recovery rate of the cryolite products and reaction pH. Influent flow: 40 L/hr, reaction temperature: 50°C, α_k = 3.00.

2.1.2 Influence of reaction temperature on the recovery rate of cryolite

Figure 3 shows the influence of reaction temperature on the recovery rate of cryolite (Run 2). The recovery rate of cryolite increases at pH 3.0 to 4.0 and retains between 72% and 82% at pH 4.0 to 7.0. Therefore, reaction temperature has minimal influence on the recovery rate of cryolite.

2.1.3 Influence of influent flow of wastewater on the recovery rate of cryolite

Figure 4 shows the influence of influent flow on the recovery rate of cryolite (Run 3). The recovery rate of cryolite reaches above 75% at an influent flow of 20 to 80 L/hr on the operation. According to Eq. (5), the stirring reaction time of cryolite varies from 56 to 14 min with increasing influent flow. Therefore, the precipitation reaction of cryolite occurs within 14 min. This result

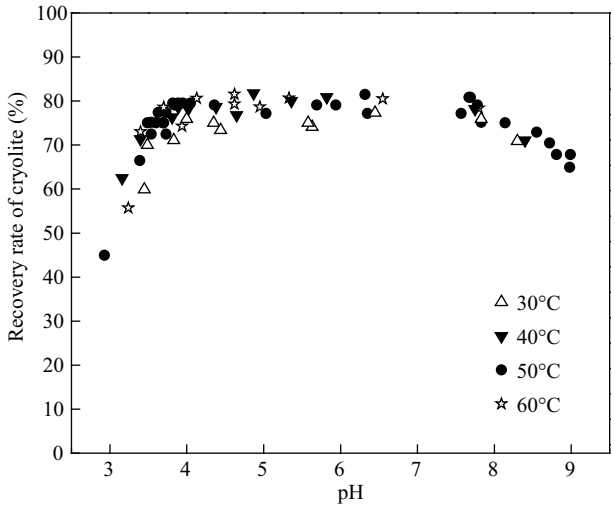

Fig. 3 Influence of temperature on the recovery rate of the cryolite products as a function of pH. Influent flow: 40 L/hr, pH: 3.0 to 9.0, α_k = 3.00.

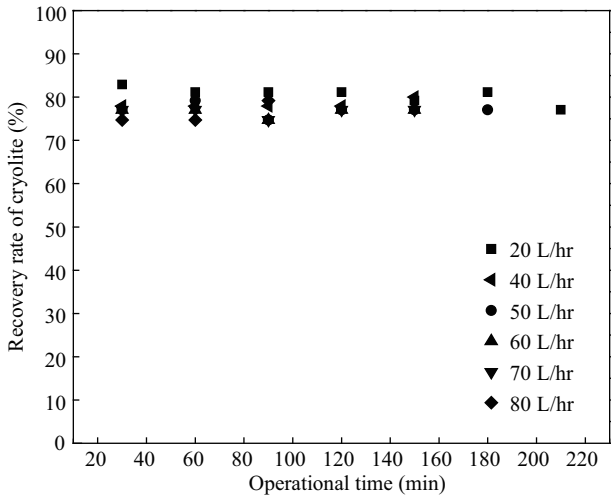

Fig. 4 Influence of influent flow on the recovery rate of the cryolite products as a function of operation time. Reaction temperature: 50°C, pH: 5.0 to 7.0, α_k = 3.00.

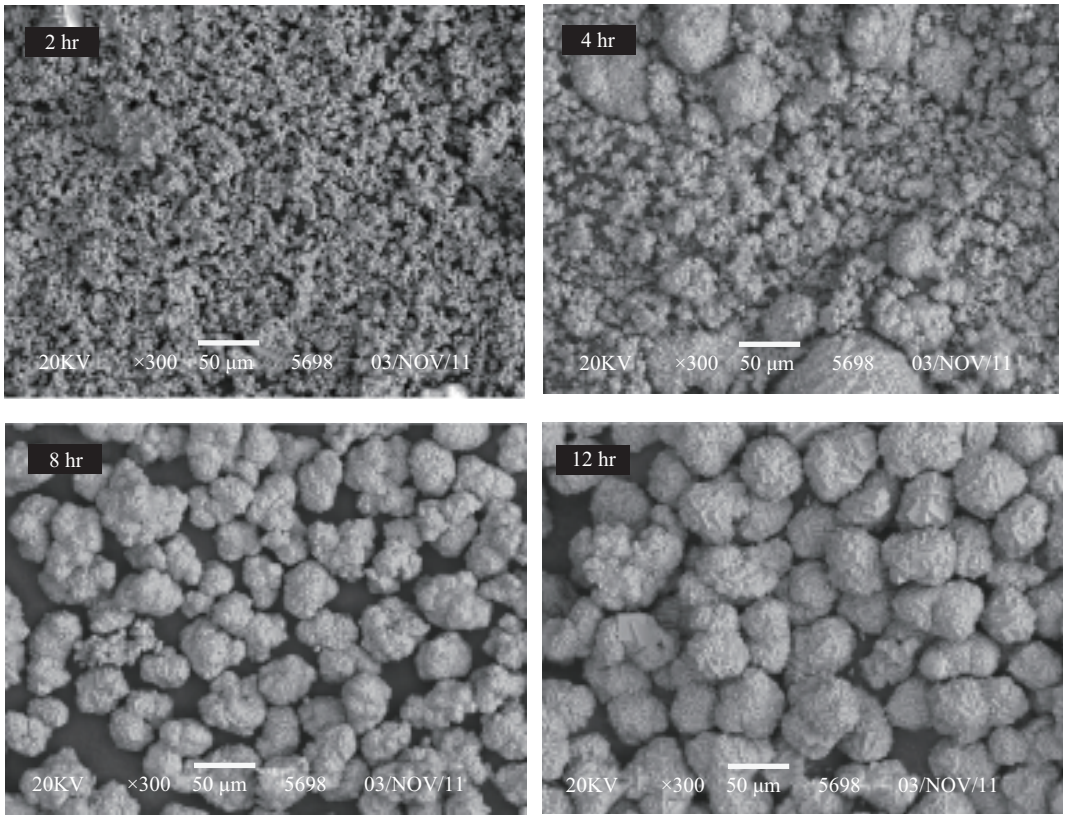

Fig. 5 SEM images of the cryolite products recovered from synthetic wastewater as a function of seed retention time (t). Influent flow: 40 L/hr, reaction temperature 50°C, pH: 5.0 to 7.0, α_k = 3.00.

indicates that stirring reaction time is not a key factor influencing the recovery rate of cryolite.

2.1.4 Influence of seed retention time on the particle size and water content of cryolite

As shown in **Fig. 5**, the fine particles of cryolite grow gradually to sandy particles with a dense surface. The particle size of cryolite increases with increasing operation time. The cryolite seed can retain on the bottom of the reactor. Therefore, the operation time is equal to seed retention time. Solution retention time and seed retention time in the integrated reactor are separated, which is the significant advantage to the traditional stirred tank reactor. As a result, the seed retention time is prolonged to strengthen the induced crystallization process at a high influent flow.

During the operation, the retention of cryolite precipitation on the bottom of the reactor forms a "seed zone" with a high solid holdup. Subsequently, fine particles are absorbed on the surface of the seed by fluid shear stress and collision/contact interaction (Ding and Tan, 1985) when passing through the "seed zone". Therefore, the fine particles grow continuously by absorption and aggregation with the seed.

Figure 6 shows the influence of particle size on the water content of cryolite. The water content of cryolite decreases from 45% to 21% with increasing particle size.

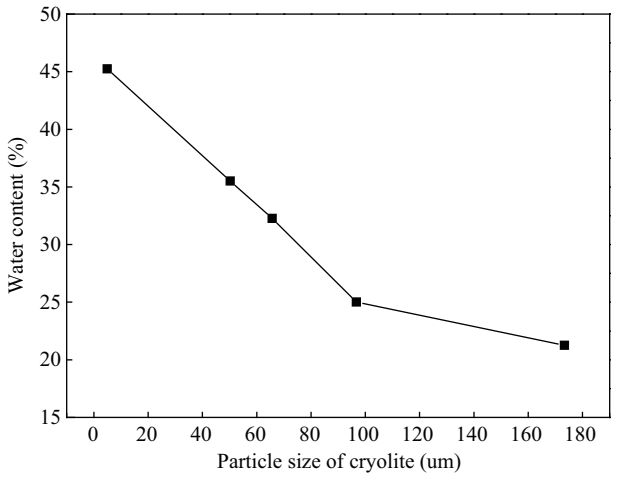

Fig. 6 Influence of particle size on the water content of the cryolite products. Influent flow: 40 L/hr, reaction temperature 50°C, pH: 5.0 to 7.0, α_k = 3.00.

If one ton dry product of cryolite is precipitated, the weight lost during the dehydration of cryolite decreases from 0.818 ton to 0.266 ton when the water content decreases from 45% to 21%. Thus, the weight lost during dehydration decreases by 67%, which indicates that the load and cost of dehydration and drying are reduced greatly.

2.2 Recovery of cryolite from industrial wastewater

2.2.1 Recovery rate of cryolite during operation

Figure 7 shows the recovery rate of cryolite during operation (Run 4). The recovery rate of cryolite increases at pH 2.5 to 4.0, and retains between 70% and 85% at pH 4.0 to 7.0, which is consistent with the phenomenon shown in **Fig. 3**. Therefore, the recovery rate of cryolite could be maintained above 70% at pH 4.0 to 7.0 during the step of using synthetic wastewater and industrial wastewater.

2.2.2 Chemical analysis of the cryolite products

Table 2 shows the quality of cryolite precipitated from industrial wastewater and National Standard of synthetic cryolite (GB/T 4291-2007) in China. As shown in **Table 2**, fluorine, aluminum, and sodium are the major components of the cryolite products, accounting for more than 52.88%, 13.39%, and less than 29.93%, respectively. In addition, silicon dioxide (SiO_2) is the main contaminant in cryolite. The amount of SiO_2 in cryolite increases from 0.12% to 0.30% with increasing α_k, which is attributed to the precipitation of Na_2SiF_6 (KopoHubIH, 1983). Compare with the Chinese National Standard of synthetic cryolite, the above chemical results of the cryolite products match very well. This finding demonstrates that the cryolite products with high quality could be used as a raw material in the aluminum electrolytic industry.

In addition, the water content of the cryolite products decreases from 35.36% to 19.30% as the molecular ratio of cryolite products increases. This result can be explained by the relationship between the species and crystal water of sodium aluminum fluoride (KopoHubIH, 1984). Generally, $Na_3AlF_6 \cdot 0.167H_2O$, $Na_5Al_3F_{14} \cdot 0.5H_2O$ and $NaAlF_4 \cdot 0.83H_2O$ are three main species of sodium aluminum fluoride. Therefore, the products with a higher molecular ratio show less crystal water and low water content.

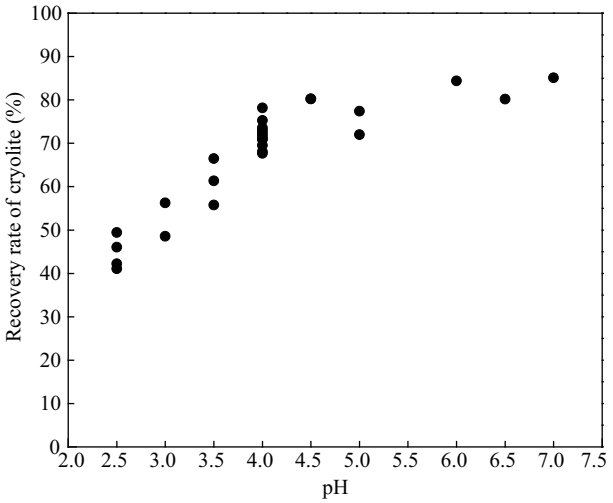

Fig. 7 Recovery rate of the cryolite products during operation. Influent flow: 40 L/hr; reaction temperature 50°C; pH: 2.5 to 7.0; α_k = 3.25.

2.2.3 SEM morphology of the cryolite products

The SEM images of the cryolite products recovered from industrial wastewater are shown in **Fig. 8**. As shown in **Fig. 8a–d**, the particle size of the cryolite increase slightly with increasing α_k in sodium aluminate, and the surface of particle becomes more dense. The cryolite product recovered in the integrated reactor is large in size, low in water content, and easy to dehydrate, which are consistent with the result shown in Section 2.1.4. In contrast, the cryolite products recovered in the stirred tank reactor are mainly composed of fine particles (**Fig. 8e**). The water content of the products is above 42%, which is attributed to the particle size of cryolite.

2.2.4 Crystal phases of the cryolite products

The phase analysises of the recovered cryolite products are shown in **Fig. 9**. The phases of the cryolite product match well with the standard phase of Na_3AlF_6. In addition, $Na_5Al_3F_{14}$ is the main contaminant of cryolite products at α_k = 1.88 to 2.95, which causes the decreasing of the molecule ratio of the cryolite products. According to the phase diagram in the $NaF\text{-}AlF_3\text{-}H_2O$ system (Lu, 1997), the high molecular ratio of cryolite is stable while the concentration of sodium fluoride is above 1% (10 g/L). This result demonstrates that the cryolite with a high molecular ratio cannot be obtained from wastewater due to its low sodium fluoride concentration.

Table 2 Chemical analysis and physical properties of the cryolite products and Chinese National Standard of synthetic cryolite (GB/T4291-2007)

No.	α_k	Temperature (°C)	F	Al	Na	SiO_2	SO_4^{2-}	Hygroscopic water	Water content of wet samples (%)	Molar ratio
a	1.88	50	≥ 53.34	≥ 15.21	≤ 25.65	≤ 0.12	≤ 0.01	0.07	35.36	1.98
b	2.45	50	≥ 54.54	≥ 14.60	≤ 25.95	≤ 0.20	≤ 0.01	0.14	27.33	2.09
c	2.95	50	≥ 54.00	≥ 13.52	≤ 29.93	≤ 0.25	≤ 0.01	0.16	23.00	2.60
d	3.25	35	≥ 52.88	≥ 13.39	≤ 29.48	≤ 0.30	≤ 0.01	0.10	19.30	2.59
CH-0			≥ 52	≥ 12	≤ 33	≤ 0.25	≤ 0.6	0.20		1.0–2.8
CH-1			≥ 52	≥ 12	≤ 33	≤ 0.36	≤ 1.0	0.40		1.0–2.8
CM-0			≥ 53	≥ 13	≤ 32	≤ 0.25	≤ 0.6	0.20		2.8–3.0
CM-1			≥ 53	≥ 13	≤ 32	≤ 0.36	≤ 1.0	0.40		2.8–3.0

No. a–d: the cryolite products recovered in the integrated reactor. No. CH-0 and CM-1: the standard samples of synthetic cryolite. The seed retention time for recovery of cryolite products (No. a–d): 5.5 hr.

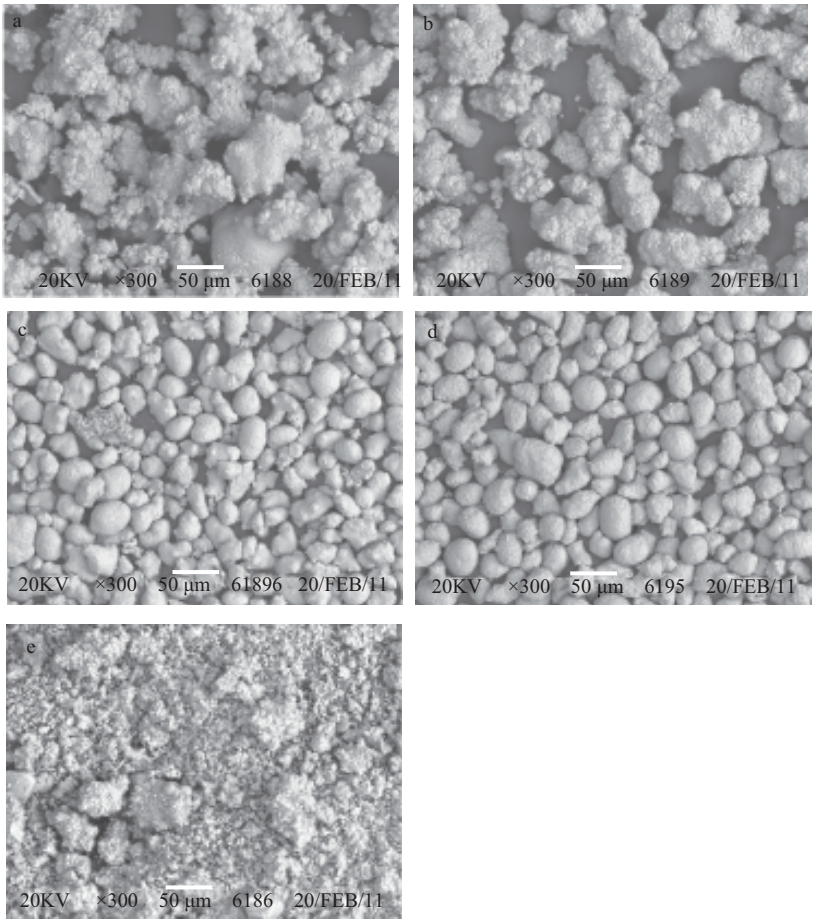

Fig. 8 SEM images of the cryolite products recovered in the reaction-separation integrated reactor, (a) α_k = 1.88; (b) α_k = 2.45; (c) α_k = 2.95; (d) α_k = 3.25 (influent flow: 40 L/hr, pH: 2.5 to 7.0); and (e) the cryolite products recovered in the stirred tank reactor of the fluoride chemical factory.

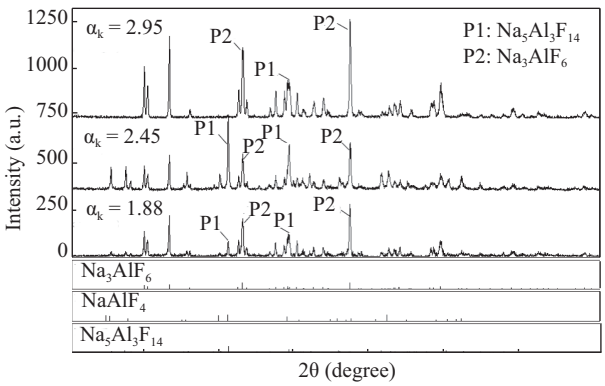

Fig. 9 XRD patterns of the cryolite products recovered from industrial wastewater. Influent flow: 40 L/hr, pH: 2.5 to 7.0.

3 Conclusions

A reaction-separation integrated reactor was designed for the recovery of cryolite with low water content from synthetic and industrial fluoride-containing wastewater. The main conclusions are as follows: The recovery rate of cryolite precipitated from synthetic wastewater is above 75% at pH 4.0 to 7.0 and 14 min stirring reaction time. The particle size of cryolite increases with increasing seed retention time, which decreases the water content. The fine particles of cryolite grow up by absorption and aggregation with the seed. The recovery rate of cryolite precipitated from industrial wastewater is above 70% at a reaction temperature of 50°C. The cryolite products with large size, low water content(< 20%), and high quality could be used as a raw material in the aluminum electrolytic industry. This result demonstrates that the recovery of cryolite with low water content is feasible in the reaction-separation integrated reactor.

Acknowledgments

This research was supported by the Major Science and Technology Program of Hunan (China) (No. 2009FJ-1009).

References

Aldaco R, Garea A, Irabien A, 2007. Calcium fluoride recovery from fluoride wastewater in a fluidized bed reactor. *Water Research*, 41(4): 810–818.

Aldaco R, Irabien A, Luis P, 2005. Fluidized bed reactor for fluoride removal. *Chemical Engineering Journal*, 107(1-3): 113–117.

Hirasawa I, Kaneko S, Kanai Y, Hosoya S, Okuyama K, Kamahara T, 2002. Crystallization phenomena of magnesium ammonium phosphate (MAP) in a fluidized-bed-type crystallizer. *Journal of Crystal Growth*, 237-239(3): 2183–2187.

Jiang K, Zhou K G, Yang Y C, Li C W, 2012. Laboratory and pilot-scale treatment of industrial fluorine-containing wastewater by fluidized bed crystallization process. *Journal of Basic Science and Engineering*, 20(6): 1032–1041.

KopoHubIH A C, 1983. The relationship between sulfate content and molar ratio of cryolite (Wang Y M, Trans.). *Light Metals*, (8): 20–22.

KopoHubIH A C, 1984. The composition of sodium aluminum fluoride (Duan X Q, Trans.). *Light Metals*, (7): 19–20.

Le Corre K S, Valsami-Jones E, Hobbs P, Parsons S A, 2009. Phosphorus recovery from wastewater by struvite crystallization: A review. *Critical Reviews in Environmental Science and Technology*, 39(6): 433–477.

Lee M S, Chang W K, Shao H, Liao C C, 2001. Volume reduction and resource recovery of fluoride-containing wastewater. In: IWA Sludge Management Entering the 3rd Millennium. Taipei, Taiwan. Vol. 44: 733–739.

Lu Z X, 1997. Synthesis and applications of the high-molecular ratio cryolite. *Light Metals*, (3): 21–24.

Meenakshi, Maheshwari R C, 2006. Fluoride in drinking water and its removal. *Journal of Hazardous Materials*, 137(1): 456–463.

Reardon, E J, Wang Y X, 2000. A limestone reactor for fluoride removal from wastewaters. *Environmental Science and Technology*, 34(15): 3247–3253.

Shi Z N, Li W, Hu X W, Ren B J, Gao B L, Wang Z W, 2012. Recovery of carbon and cryolite from spent pot lining of aluminium reduction cells by chemical leaching. *Transactions of Nonferrous Metals Society of China*, 22(1): 222–227.

Turner B D, Binning P, Stipp S L S, 2005. Fluoride removal by calcite: Evidence for fluorite precipitation and surface adsorption. *Environmental Science and Technology*, 39(24): 9561–9568.

Wang L S, Wang C M, Yu Y, Huang X W, Long Z Q, Hou Y K et al., 2012. Recovery of fluorine from bastnasite as synthetic cryolite by-product. *Journal of Hazardous Materials*, 209-210: 77–83.

Wu J, Lu Z Y, 2003. Combined treatment process for high fluoride content wastewater. *China Water and Wastewater*, 19(S1): 39–40.

JOURNAL OF ENVIRONMENTAL SCIENCES

环境科学学报(英文版)

(http://www.jesc.ac.cn)

Aims and scope

Journal of Environmental Sciences is an international academic journal supervised by Research Center for Eco-Environmental Sciences, Chinese Academy of Sciences. The journal publishes original, peer-reviewed innovative research and valuable findings in environmental sciences. The types of articles published are research article, critical review, rapid communications, and special issues.

The scope of the journal embraces the treatment processes for natural groundwater, municipal, agricultural and industrial water and wastewaters; physical and chemical methods for limitation of pollutants emission into the atmospheric environment; chemical and biological and phytoremediation of contaminated soil; fate and transport of pollutants in environments; toxicological effects of terrorist chemical release on the natural environment and human health; development of environmental catalysts and materials.

For subscription to electronic edition

Elsevier is responsible for subscription of the journal. Please subscribe to the journal via http://www.elsevier.com/locate/jes.

For subscription to print edition

China: Please contact the customer service, Science Press, 16 Donghuangchenggen North Street, Beijing 100717, China. Tel: +86-10-64017032; E-mail: journal@mail.sciencep.com, or the local post office throughout China (domestic postcode: 2-580).

Outside China: Please order the journal from the Elsevier Customer Service Department at the Regional Sales Office nearest you.

Submission declaration

Submission of an article implies that the work described has not been published previously (except in the form of an abstract or as part of a published lecture or academic thesis), that it is not under consideration for publication elsewhere. The submission should be approved by all authors and tacitly or explicitly by the responsible authorities where the work was carried out. If the manuscript accepted, it will not be published elsewhere in the same form, in English or in any other language, including electronically without the written consent of the copyright-holder.

Submission declaration

Submission of the work described has not been published previously (except in the form of an abstract or as part of a published lecture or academic thesis), that it is not under consideration for publication elsewhere. The publication should be approved by all authors and tacitly or explicitly by the responsible authorities where the work was carried out. If the manuscript accepted, it will not be published elsewhere in the same form, in English or in any other language, including electronically without the written consent of the copyright-holder.

Editorial

Authors should submit manuscript online at http://www.jesc.ac.cn. In case of queries, please contact editorial office, Tel: +86-10-62920553, E-mail: jesc@263.net, jesc@rcees.ac.cn. Instruction to authors is available at http://www.jesc.ac.cn.

Journal of Environmental Sciences (Established in 1989)

Vol. 25 No. 7 2013

Supervised by	Chinese Academy of Sciences	**Published by**	Science Press, Beijing, China
Sponsored by	Research Center for Eco-Environmental		Elsevier Limited, The Netherlands
	Sciences, Chinese Academy of Sciences	**Distributed by**	
Edited by	Editorial Office of Journal of	Domestic	Science Press, 16 Donghuangchenggen
	Environmental Sciences		North Street, Beijing 100717, China
	P. O. Box 2871, Beijing 100085, China		Local Post Offices through China
	Tel: 86-10-62920553; http://www.jesc.ac.cn	Foreign	Elsevier Limited
	E-mail: jesc@263.net, jesc@rcees.ac.cn		http://www.elsevier.com/locate/jes
Editor-in-chief	Hongxiao Tang	**Printed by**	Beijing Beilin Printing House, 100083, China

CN 11-2629/X **Domestic postcode: 2-580** **Domestic price per issue RMB ¥ 110.00**

ISSN 1001-0742